HAPTIC RENDERING FOR VR LAPAROSCOPIC SURGERY SIMULATION

Ryan McColl, Ian Brown, Cory Seligman, Fabian Lim, Amer Alsaraira

Electrical and Computer Systems Engineering, Monash University, Clayton, Victoria, 3800, Australia

ryan.mccoll@eng.monash.edu.au

Abstract

This project concerns the application of haptic feedback to a VR laparoscopic surgery simulator. Haptic attributes such as mass, friction, elasticity, roughness and viscosity are individually modeled, validated and applied to the existing visual simulation created by researchers at Monash University. Haptic feedback is an essential element in an immersive and realistic virtual reality laparoscopic training simulator. The haptic system must display stable, continuous and realistic multi-dimensional force feedback, and its inclusion should enhance the simulators training capability. Stability is a recurring concern throughout haptic history, and will be tackled with the implementation of a stable control algorithm and a passive environment model.

Haptic force feedback modeling, systems implementation and validation studies form the principal areas of new work associated with this project.

Key words: Haptic, Force Feedback, Surgery Simulation, Laparoscopy and Virtual Reality

Introduction

The sense of touch provides useful information to surgeons when they are orientating themselves, diagnosing pathologies and manipulating tissue. Despite the use of touch being of secondary importance to that of vision, in order to ensure a completely immersive and realistic VR simulator, haptic feedback must be included. Due to computing power issues in the past, the implementation and development of a haptic feedbacksystem has come secondary to the highly computationally expensive visual graphic components. Improvements in technology and further research, will enable haptic feedback to become more reliable, stable and commonplace. It is currently used in various simulations such as Cathoder Insertion [1], Prostate Palpation [2] and Laparoscopic Procedures [3] [4] [5] [6] [1] [7].

Overview of Current Research

Following on from the development of the haptic mechanical interface designed by Seligman [8] [9], the construction of a third prototype has been undertaken. Figure 1 shows the new mechanical interface. In terms of the software modeling, the coordinate system has been defined and simple procedures have been written to validate the ability for the interface to display a 3D force to the user. An initial validation study has been undertaken in which a number of subjects have been tested to determine their ability to find the apex of a virtual sphere. The results of this work are found in Section 5.
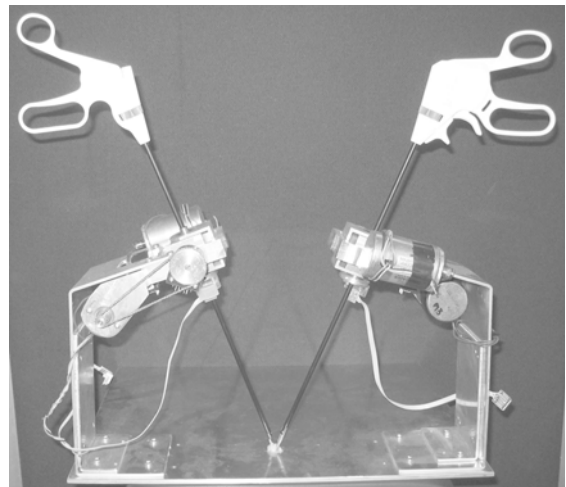

Figure 1. *The Mechanical Interface.*

Systems Model

Figure 2 provides an overview of the project in terms of information flow and I/O paths. The system has three major components: the Human Operator, the Haptic Device, and Haptic Control and Virtual Environment Model. It should be noted that the flow of information through the control system simultaneously occurs in 3 dimensions.

Haptic Force Feedback DC Motors

Motors

Haptic motors are a subject of current research and design consideration.

Haptic Force Feedback DC Motors

Motors

Haptic motors are a subject of current research and design consideration.

Despite the active position control and frictional benefits of the brushless DC motor, the regular brush type DC motor is initially being used because of the price benefits and simpler control circuitry required.
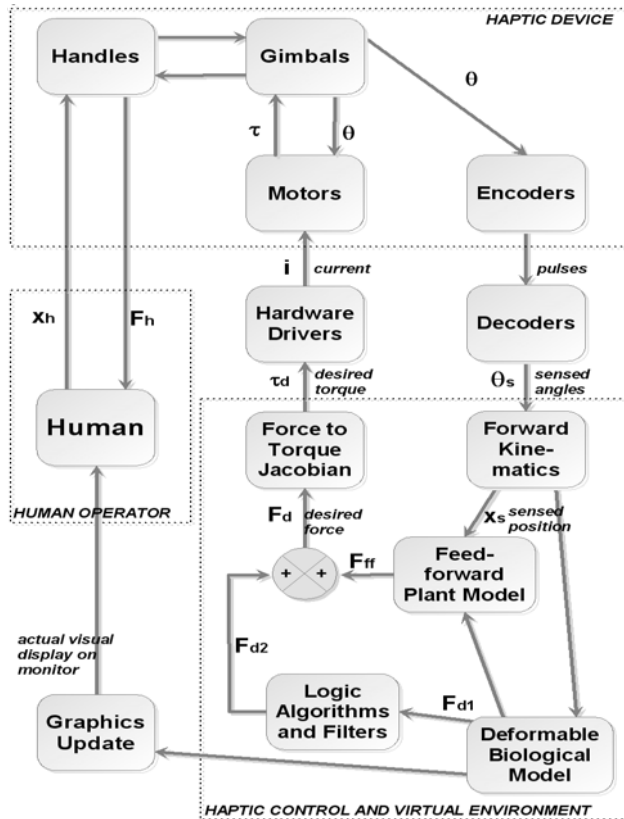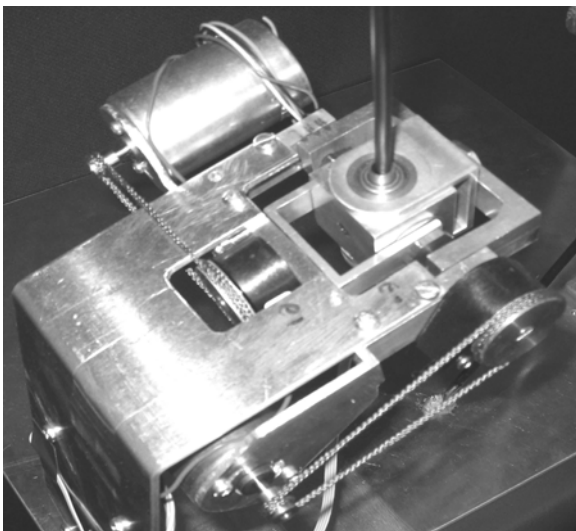
Figure 2. *Block Diagram - System Overview.*

Figure 3. Overview of Gimbal.

Amplifiers

The torque required to enable the user to feel as though they have contacted a solid object is the main consideration in determining how much amplification is required for the motors. The top rotational speed is irrelevant because the motors generally operate at near stall, and mechanical design limitations ensure that the shafts rotate little more than 360o. Previous torque tests deemed it necessary to ensure the motor driving currents were least ±2.5A. Tests have shown that this current can

be used to display continual forces of approximately 3N in 3 dimensions, which is within the normal ranges as felt by laparoscopic surgeons [10] [11].

Power Supply

From prior calculations of torque requirements and amplifier constraints, the power supply to the ampli-fiers needs to be about ±40V. Power transfer in haptics is generally not continuous, so the power rating need not be as high as the maximum continual power rating of all DC motors on board one mechanical interface set. The power supply needs to be large enough to supply up to 9 DC motors. No off the shelf power supply was available for this task, so a unique one was designed with a 160VA 30V CT toroidal coil. Sufficient capacitance was added to remove ripple to negligible amounts.

Mechanical Interface

The mechanical interface is based on previous work but has had a number of improvements made. An overview of the gimbal construction and how it connects to the force feedback motors and mounting arm are shown in Figure 3.

Improved Range of Motion: The gimbals were refined to allow greater range of movement. This increases the volumetric workspace available for simulation purposes.

Flexible Mounting Options: Provision was made for the positions of the three instruments to be mounted in various locations allowing for changes in surgeon preference and for various operational procedures. The new mounting scheme also allows the addition of a third and fourth instrument as required.

Analogue Clamping: The grasper handle has been fitted with a potentiometer to allow continual tracking of the grasper position.

Rotational Monitoring: 4 Dimensional positioning is now available with the introduction of rotational monitoring. An Agilent/HP HEDR-8000 [12] Reflective Optical Surface Mount Encoders was added to the design giving _ 1o degree resolution.

Hardware/Software Interface: The hardware/software interface was designed to allow fast information flow between the computer, the motor amplifiers and the shaft encoders. Communication speeds of approximately 1000Hz are necessary for a satisfactory haptic display [13]. The PCB is a unique design with the major components being a USB device from FTDI [14], a microcontroller and D-A converter from Maxim [15] and decoder chips from US Digital [16]. The microcontroller has been programmed to relay information between the USB device and the D-A converters and the decoder chips. The high information transfer rate from the PC ensures that no haptic calculations or interpolation need

to occur on board the microcontroller. These calculations are done in the PC, which reduces development time and data packet sizes. The PC programming is written for Linux and interfaces directly with the USB. Tuning of the microcontroller clock speed, USB transfer methods, USB buffer sizes, driver classes and thread priorities have enabled the transfer of 64kByte packets at consistent speeds between 800-1000Hz.

Preliminary Validation

Initial tests were undertaken to ensure the haptic device was able to display continual stable forces in 3 dimensions with magnitudes of up to approximately 3N. A study was undertaken to determine if the improvements made to the interface actually improved its haptic performance. The study involved subjects finding the apex of a virtual hemisphere placed randomly on a virtual horizontal plane using the haptic instrument. The virtual hemispheres radius was kept constant at 20mm, the same as a table tennis ball. Once the subject found the apex of the hemisphere, the tester stopped the simulation, recording the subjects coordinate values. Each subject was tested on 10 virtual hemispheres and 5 subjects in total were tested. To maintain consistency with previous results, the error of the subjects attempt to find the apex was calculated as a percentage of the radius for both the x and y axis. The mean error was 14.2% with the standard deviation 11.3. This suggests a marked improvement from previous results (mean error of 29.7%) indicating that the new haptic interface, with increased force capabilities, greatly improves a users ability to navigate a virtual environment. A plot of results can be found in Figure 4.

Haptic Modeling

Haptic modeling consists of the creation of models to generate virtual haptic forces, the realisation of these models, and model validation in the context of the overall simulation.
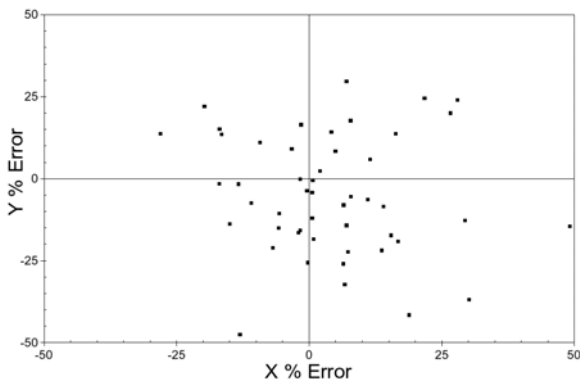

Figure 4. *% Error In Locating Virtual Spheres.*

Coordinate System

The gimbal allows instrument movement in four degrees of freedom (H,P,R,D). In the current hardware implementation, the H axis (heading) reflects rotation of the instrument left and right, the P axis (pitch) represents rotation forward and back, the R axis (roll) represents rotation of the handle about its own axis and the D axis (depth) represents axial movement of the instrument through the centre of the gimbal. Cartesian coordinates (X,Y,Z) are used by the visual loop and relationships must be made in order to pass information between visual and haptic loops. A Cartesian normal surface vector is passed from the visual loop when contact is made between an instrument and an object. This is converted to a force vector based on attributes of the organ, such as mass or deformation. In order to display this force to the user through the mechanical interface, the Cartesian vector must be separated into their polar coordinates, which allows the signal for the feedback motors to be generated. The final relationships are detailed below, and proof of the formulas can be found in [8]. The coordinate system adopted is detailed in Figure 5.

$$Fh = Fxcos(h) - Fzsin(h)$$

$$Fp = Fycos(p) - Fzsin(p)$$

$$Fd = Fxsin(h) + Fysin(p) + Fzcos(h)cos(p)$$

Object Orientated Modeling

The initial models will be based on a simple object orientated approach which lends itself nicely to the addition of new objects and features into the VR model. Listed is a set of basic haptic attributes that can be used as building blocks to define the properties of particular objects. Attributes, such as elasticity, mass, deformation, roughness, friction and viscosity need to be modeled in software and then validated using human subjects. The individual attributes can then be combined to create the overall properties of an anatomical object. An ovary, for example, has the individual attributes of mass, deformability, roughness and friction.
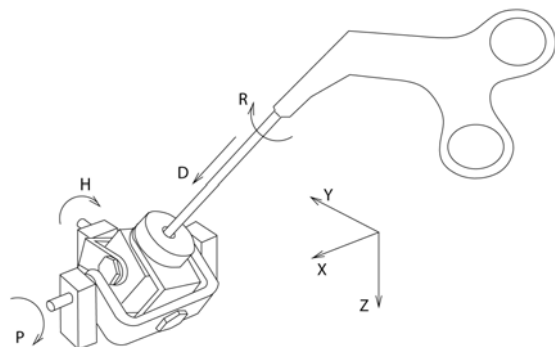

Figure 5. *The Coordinate System.*

Passive Object Modeling

Passive object models are necessary to ensure stable operations. Physically based models monitor energy changes of the entire object to calculate deformations, so it is given that the object does not itself generate energy. Physical models are currently too computationally demanding for a laparoscopic trainer. The geometric visual models used by the haptic loop must be made physical in some simple way in order to monitor energy changes. It is proposed to monitor each point of the object being contacted to determine whether it has moved from its initial position. If moved, it will have stored energy based on the extension of the spring-damper model developed. Actively comparing the energy displayed to the user and the change of energy stored in the object, should enable the geometric model to remain passive.

Elastic Tube Model

The elastic tube model will be first based on a simple elastic model. Fixed at one end, mass will be neglected, and the forces felt will oppose motion proportional to the distance stretched. Although this is not an accurate representation of tissue biomechanics, non-linear attributes may be added at a later stage. The fallopian tube is an example of where this model will be used.

Mass Model

The property of weight is simply the mass of the object multiplied by gravity, or mg. It is a unidirectional constant force and can be represented as polar forces by subsituting into the formulas given in Section 6.1.

$$Fh = mg.sin(h)$$

$$Fp = mg.sin(p)$$

$$Fd = mg.cos(h).cos(p)$$

The forces associated with accelerating a mass, ma, will be investigated but are currently believed to be negligible. This is due to the small masses of objects and slow acceleration rates encountered during laparoscopic surgery. For example, the mass of an ovary is approximately 10 grams.

Deformation Model

Deformation will be handled in a similar way to the elastic tube discussed in Section 6.4. Using data available from the visual model, forces will initially be normal to the surface and proportional to the distance from the original surface position. This will be improved by implementing a local data set in the haptic loop to improve fidelity. A force continuum algorithm will be implemented to ensure smooth transitions whilst sliding the tool tip between two segments of the object model.

Roughness, Friction and Viscosity Models

At the simplest level, roughness can be modeled using a random white noise type function, frictional forces opposes motion perpendicular to the surface normal, and viscosity forces opposes motion with a force proportional to velocity. These will be further developed with surgeon feedback and following some guidelines from [17] and [18].

Related Research

Haptic-Visual Graphic Integration

The surfaces to be haptically rendered are created using the existing graphical models and there is thus no need to construct separate haptic models for the anatomical objects. When the graphical loop detects that a collision between an instrument and an object has occurred, it passes both the surface normal and depth of depression (or length of extension) to the haptic loop. The haptic loop uses this information and visco-elastic properties of the object to calculate individual polar force vectors. The visual loop is refreshed at 30Hz, whereas the haptic loop needs to operate at about 1000Hz. Interpolation is therefore necessary to maintain a stable haptic output. The haptic loop continually collects position data from the shaft encoders and predicts what the objects responses will be. After a visual loop update, the haptic loop compares predicted values and the process repeats. The haptic attributes of elasticity, mass, roughness, friction, etc., are developed in order to provide a haptic dimension to a visual graphic VR model. It is therefore necessary to apply these attributes to various anatomical objects as required. This application will take the form of mapping (or haptic rendering). The models developed to provide output to the haptic motors will need to be assessed in relation to each anatomical object. Additionally the deformation and modification (i.e. cutting) of an anatomical object will need to be synchronised to the haptic response.Once the haptic attributes are modeled and work sufficiently well with the hardware and test programs, they will be integrated in Mayooran's [19] visual model known as Virtual Kylie. Implementing haptics onto this model will achieve the milestone of giving a user a chance to immerse themselves into an interactive virtual female abdominal cavity.

Deformation

When the instrument moves between two adjacent segments, the surface normal, and thus the direction of the desired force vector will change instantaneously. A method for ensuring smooth and continuous force display is described below and visualised in Figure 6.

• The vectors A and B are surface normals for two adjacent triangular segments.

• The vectors 1,2,3 and 4 are normals averaged from the surrounding segments. For simplicity, only 2 segments are shown in Figure 6. Vector 2, for example, is the average of surface normals A and B (it would also take into account the other adjacent segments not shown in this example).

• To calculate the desired force vector F, a weighted average of the 3 point normals of the contacted segment (in this case, F equals the weighted average of 1,2 and 3) is calculated, where the weighting is dependent on the point location on the segment.

• In the example, when the tool is on the intersection line between segments A and B, the vectors 1 and 4 have no effect on the resultant force vector. Therefore there is a smooth transition between segments.

Since these calculations will be performed in the haptic loop, the graphics loop must pass on not only information for the segment being contacted, but also for all adjacent segments. This information can also be used for the haptic interpolation. One limitation of the above method is that objects with hard edges will be haptically rendered as having rounded edges. This is not an issue because anatomical objects are generally smooth and continuous.
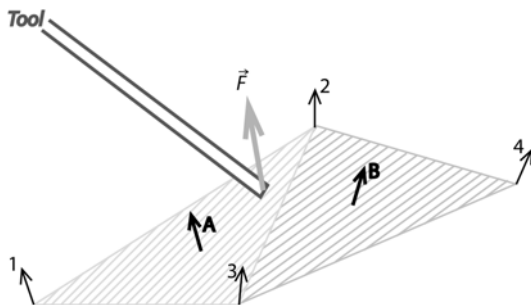

Figure 6. *Calculating Forces.*

Control Algorithm for Multiple Instruments

Multiple instrument modeling becomes a requirement when two or more instruments interact on the same object. For example, take the simple case of holding an unfixed elastic tube between two instruments as shown in Figure 7. There are no fixed boundary conditions so good control methods become critical. The unknown nature of the human element is also magnified because there are now multiple occurrences of the human block in the control loop. Multiple instrument interaction will provide an excellent basis for establishing system stability under worst case conditions.

Figure 7. *Multiple Instrument Interaction.*

Dynamic Plant Model

The feedforward model will firstly incorporate the mass of the gimbal and instrument. Inertia should be small enough to be negligent due to the small velocities encountered during surgery of this type, but will be considered. To remove the effect of friction, a method similar to Tholey et al [11] will be adopted - that is, by moving the motors at low velocities, we can assume that the torque required to cause the movement is the frictional torque in the mechanism. Their measurements were for only 1 dimension, so for this project, the motion through multiple directions and the effect of mass will be tested and incorporated respectively.

It may be possible to futher advance this model over time to include some pre-calculated situations for smoother operation. For example, if the tool tip hit a solid object whilst moving at 5m/s at 30o to the normal, what is the best way to control the motor torque to get the most realistic response? The solution to this may also constitute part of the object control model.

Validation

Psychophysics Studies

To validate the haptic features it is essential to undertake psychophysics studies to determine whether each feature is perceptible and effective. Listed below are validation studies that are currently being undertaken.

• **Elastic Tube:** The virtual elastic tube will be fixed at one end to the virtual floor, and fixed to the grasper at the other end. 3 virtual tubes will be modeled, each of varying stiffness. The subject will be given the 3 tubes to test, rating them in order of stiffness. This will be repeated with tubes of various stiffnesses until the smallest incremental stiffness change determinable is found.

• **Mass:** As with the elastic tube tests, subjects will be given 3 virtual objects, to rate in terms of lightest to heaviest. This will determine to what level mass is discrimination possible.

• **Deformation:** 3 objects, each with varying stiff-ness properties, will be tested to determine to what level object stiffness discrimination is possible.

• **Roughness,** Friction & Viscosity: Similar tests to above.

Surgeons Study

In addition to testing individual haptic attributes there is a need to validate these characteristics in the context of the overall visual graphic model. This will be undertaken with laparoscopic surgeons as subjects and will involve a quantitative evaluation.

Conclusion

The researchers are currently engaged in the introduction of haptics into a virtual reality based laparoscopic simulator. The development of haptic rendering hardware and software has identified a number of important engineering design challenges. Solutions to these challenges need to be both cost effective and computationally efficient. Global physical modeling may produce a single virtual organ with realistic visual and haptic properties but a multi-organ, multi-instrument, multioperator simulation suggests a less global, more segmented object orientated approach. This approach is currently being investigated in relation to the haptic rendering of a VR laparoscopic simulator.

References

[1] [Online]. Available: http://www.immersion.com
[2] G. Burdea, G. Pataounakis, V. Popescu, andR. E. Weiss, "Virtual Reality-Based Training for the Diagnostics of Prostate Cancer," IEEE Trans. Biomed. Eng., vol. 46, no. 10, pp. 1253–1260, Oct. 1999.
[3] [Online]. Available: http://www.surgical-science.Com
[4] [Online]. Available: http://www.xitact.com
[5] [Online]. Available: http://www.mentice.com
[6] [Online]. Available: http://www.reachin.se
[7] G. Burdea and P. Coiffet, Virtual Reality Technology - 2nd Edition. Wiley, 2003.
[8] C. Seligman, "Force Feedback Haptics for Virtual Reality Laparoscopic Surgery," Master's thesis, Monash University, Department of Electrical and Computer Systems Engineering, Clayton, Australia, 2003.
[9] I. Brown, C. Seligman, Z. Mayooran, and D. Healy, "Haptic Rendering In A Virtual Reality Based Endoscopic Simulator," in Engineering and the Physical Sciences in Medicine. Geelong, Australia: EPSM, 2004.
[10] I. Brouwer, J. Ustin, L. Bentley, A. Sherman, N. Dhruv, and F. Tendick, "Measuring In Vivo Animal Soft Tissue Properties for Haptic Modeling in Surgical Simulation," in Medicine Meets Virtual Reality. MMVR, 2001, pp. 69–74.
[11] G. Tholey, T. Chanthasopeephan, T. Hu, J. P. Desai, and A. Lau, "Measuring Grasping and Cutting Forces for Reality-Based Haptic Modeling," in Computer Assisted Radiology and Surgery - 1st International Workshop on Haptic Devices in Medical Applications, London, UK, 2003, pp. 794–800.
[12] [Online]. Available: http://www.agilent.com/
[13] C. Basdogan, "Force-Reflecting Deformable Objects for Virtual Environments," sig9902.html, June 2004. [Online]. Available: http: //network.ku.edu.tr/_cbasdogan/Tutorials/
[14] [Online]. Available: http://www.ftdichip.com
[15] [Online]. Available: http://www.maxim-ic.com/
[16] [Online]. Available: http://www.usdigital. com/
[17] V. Hayward and B. Armstrong, "A New Computational Model of Friction Applied to Haptic Rendering," in Experimental Robotics VI, P.I. Corke and J. Revelyan (Eds.). Springer: New York, 2000.
[18] M. Mahvash and V. Hayward, "High-Fidelity Haptic Synthesis of Contact with Deformable Bodies," IEEE Comput. Graph. Appl., vol. 24, no. 2, pp. 48–55, Mar./Apr. 2004.
[19] Z. Mayooran, "Development of a VR Simulator for Gynaecological Endoscopy," Ph.D. dissertation, Monash University, Department of Electrical and Computer Systems Engineering, Clayton, Australia, 2003.

NONINVASIVE DETECTION OF BILIRUBIN USING PULSATILE ABSORPTION

Mark McEwen[1,2], Karen Reynolds[1]

[1]*School of Informatics and Engineering, Flinders University*
[2]*Flinders Biomedical Engineering, Flinders Medical Centre, Adelaide, Australia*
Mark.McEwen@flinders.edu.au

Abstract

Bilirubin, the yellow substance usually responsible for neonatal jaundice, is currently monitored invasively or by observing/measuring skin colour. This paper investigates the feasibility of monitoring serum bilirubin concentration using light absorbance in a similar fashion to pulse oximetry. The light absorbance of bilirubin is shown to be sufficiently different to haemoglobin to in theory allow direct noninvasive serum bilirubin monitoring using light absorbance around 480nm.

Key words: Bilirubin, noninvasive, absorption, pulse oximetry, haemoglobin, Beer Lambert law.

Introduction

Oxygenated and reduced haemoglobin are major absorbers of visible and near infrared light in blood. This strong light absorbance is exploited in pulse oximetry where the ratio of oxygenated to total haemoglobin is determined, based on the ratio of light absorbance at 2 different wavelengths. Theoretically, the Beer Lambert law states:

$$\frac{I_o}{I_i} = e^{-\varepsilon c d} \qquad \text{equation 1}$$

$$\text{Absorbance} = \ln\left(\frac{I_i}{I_o}\right) = \varepsilon c d \qquad \text{equation 2}$$

$$\therefore \text{Concentration} = \frac{\text{Absorbance}}{\varepsilon d} \qquad \text{equation 3}$$

Where:

I_o = Light intensity leaving a non scattering light absorbing solution
I_i = Light intensity entering a non scattering light absorbing solution
ε = Absorption coefficient of light by the absorbing substance ($L.mol^{-1}cm^{-1}$)
c = concentration of absorbing substance in the solution ($mol.L^{-1}$)
d = Light pathlength through the solution (cm)

If base-10 logarithms are used, equation 2 becomes:

$$\log_{10}\left(\frac{I_i}{I_o}\right) = \frac{\varepsilon c d}{\ln(10)} \qquad \text{equation 4}$$